nature COMMUNICATIONS

ARTICLE

https://doi.org/10.1038/s41467-019-08967-8 OPEN

Metal-free dehydropolymerisation of phosphine-boranes using cyclic (alkyl)(amino)carbenes as hydrogen acceptors

Nicola L. Oldroyd [1], Saurabh S. Chitnis [1,2], Vincent T. Annibale [1], Marius I. Arz [1], Hazel A. Sparkes[1] & Ian Manners[1,3]

The divalent carbene carbon centre in cyclic (alkyl)(amino)carbenes (CAACs) is known to exhibit transition-metal-like insertion into E–H σ-bonds (E = H, N, Si, B, P, C, O) with formation of new, strong C–E and C–H bonds. Although subsequent transformations of the products represent an attractive strategy for metal-free synthesis, few examples have been reported. Herein we describe the dehydrogenation of phosphine-boranes, $RR'PH{\cdot}BH_3$, using a CAAC, which behaves as a stoichiometric hydrogen acceptor to release monomeric phosphinoboranes, $[RR'PBH_2]$, under mild conditions. The latter species are transient intermediates that either polymerise to the corresponding polyphosphinoboranes, $[RR'PBH_2]_n$ (R = Ph; R′ = H, Ph or Et), or are trapped in the form of CAAC-phosphinoborane adducts, $CAAC{\cdot}H_2BPRR'$ (R = R′ = *t*Bu; R = R′ = Mes). In contrast to previously established methods such as transition metal-catalysed dehydrocoupling, which only yield P-monosubstituted polymers, $[RHPBH_2]_n$, the CAAC-mediated route also provides access to P-disubstituted polymers, $[RR'PBH_2]_n$ (R = Ph; R′ = Ph or Et).

[1] School of Chemistry, University of Bristol, Cantock's Close, Bristol BS8 1TS, UK. [2] Department of Chemistry, Dalhousie University, 6274 Coburg Road, P.O. 15000, Halifax, NS B3H 4R2, Canada. [3] Department of Chemistry, University of Victoria, Victoria, BC V8W 3V6, Canada. Correspondence and requests for materials should be addressed to I.M. (email: imanners@uvic.ca)

Polymers that feature *p*-block elements other than carbon in the main chain are interesting materials due to their potential uses as elastomers, etch resists in lithography, polyelectrolytes, ceramic precursors and in optoelectronics[1–4]. Earlier syntheses of inorganic polymers were achieved by the use of polycondensation and ring-opening methods[1,2,5]. Access to stable yet reactive, polymerisable, multiply bonded *p*-block monomers required for addition polymerisation remains a major challenge in the synthesis of inorganic polymers[6–8]. More recently, metal-catalysed coupling routes have been developed for accessing a broad range of inorganic macromolecules and materials[2,9–14]. In this context catalytic dehydrocoupling between main-group substrates has been shown to be a versatile method for the general formation of E–E′ bonds, which can be also used to access polymers via catalytic dehydropolymerisation[15–20].

Polyphosphinoboranes attracted initial interest in the 1950s as a result of their potential as flame-retardant materials with high thermal stability[21–23]. However, attempts to dehydrocouple phosphine-borane adducts under thermal conditions yielded either low molecular weight or poorly soluble materials, which lacked convincing structural characterisation by modern standards[2,24,25]. Since 1999 a rhodium-catalysed dehydrocoupling approach to prepare soluble, high-molecular-weight (P-monosubstituted)polyphosphinoboranes has been available[26–28]. Examples of iron and iridium-catalysed dehydrocouplings have also been reported as routes to high-molecular-weight poly(arylphosphinoboranes) (Fig. 1a)[29,30]. Notably, these transition metal-catalysed protocols all require forcing conditions (≥100 °C, ≥20 h) and their scope is currently limited to the dehydrocoupling of primary arylphosphine-boranes, $RPH_2{\cdot}BH_3$ (R = aryl). More recently, from our collaboration with Scheer and co-workers[31,32], a metal-free synthesis of polyphosphinoboranes through the thermolysis of amine-stabilised phosphinoboranes, $RR'PBH_2{\cdot}NMe_3$, was reported to proceed under milder conditions 22–40 °C. This route successfully produced high-molecular-weight poly-*tert*-butylphosphinoborane, $[tBuHPBH_2]_n$, presumably via the monomeric phosphinoborane $[tBuHPBH_2]$. However, the precursors are challenging to prepare and attempts to access the P-disubstituted poly(diphenylphosphinoborane), $[Ph_2PBH_2]_n$, by the thermolysis of $Ph_2PBH_2{\cdot}NMe_3$, yielded only very-low-molecular-weight oligomers $[Ph_2PBH_2]_x$ ($x \leq 6$) (Fig. 1b). The development of convenient and efficient dehydrocoupling of secondary phosphine-borane adducts to give the corresponding polymers therefore remains an open challenge. Herein, we demonstrate the successful use of the carbene centres of cyclic (alkyl)(amino)carbenes (CAACs) to mediate this process.

CAACs are analogues of *N*-heterocyclic carbenes (NHCs) with one of the electronegative amino substituents replaced by a strong σ-donating alkyl group, which simultaneously increases the nucleophilicity and electrophilicity at the divalent carbene carbon centre[33–36]. The resulting small HOMO–LUMO gap of CAACs has allowed E–H (E = H, N, Si, B, P, C, O) bond activation by formal oxidative addition to the carbene carbon centre for a variety of small molecules under mild conditions, with this process giving products featuring a H–C(sp^3)–E moiety[37–42]. However, the strength of the resulting C(sp^3)–H and C(sp^3)–E σ—bonds disfavours further reactivity of the H–C(sp^3)–E products, limiting the ability of CAACs to mimic transition metal centres in synthetic utility.

We envisioned that a CAAC-mediated dehydrogenation of primary and secondary phosphine-boranes, species that contain both protic P–H and hydridic B–H bonds, may be possible (Fig. 1c). Dehydrogenation of phosphine-boranes using this strategy leads to reactive phosphinoborane monomers, which, given appropriate substituents at the phosphorus and boron centres, gives soluble oligomeric and polymeric material.

Results

Reactivity of carbenes with phosphine-boranes. The synthesis of monomeric aminoborane-NHC adducts (NHC-BH_2NHR) has been reported both through the use of an NHC for ambient temperature dehydrogenation of amine-boranes ($RNH_2{\cdot}BH_3$; R = H, Me)[43] and NHC-induced depolymerisation of poly (*N*-methylaminoborane)[44]. More recently, analogous species featuring the use of NHCs to stabilise phosphinoborane monomers have been isolated using NHC-induced thermal depolymerisation of polyphosphinoboranes[45]. Consequently, prior to investigating the reactivity of phosphine-boranes with CAACs, we explored the dehydrogenation potential of NHCs.

Upon addition of one equivalent of IDipp to a solution of $PhPH_2{\cdot}BH_3$ in tetrahydrofuran (THF), a homogeneous solution was formed after 10 min, and analysis of the reaction mixture by ^{31}P

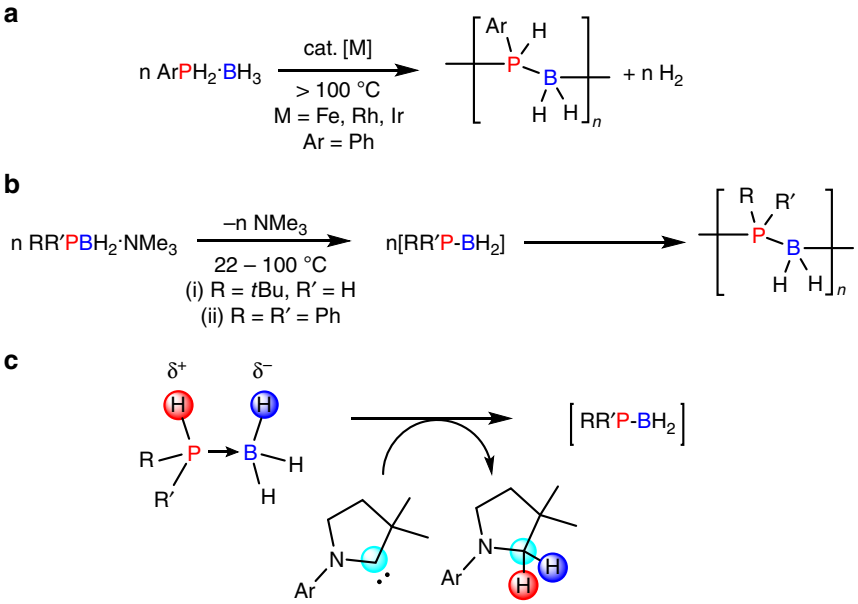

Fig. 1 Synthesis of polyphosphinoboranes. **a**, **b** Current methods of synthesis and **c** proposed CAAC-mediated dehydrogenation

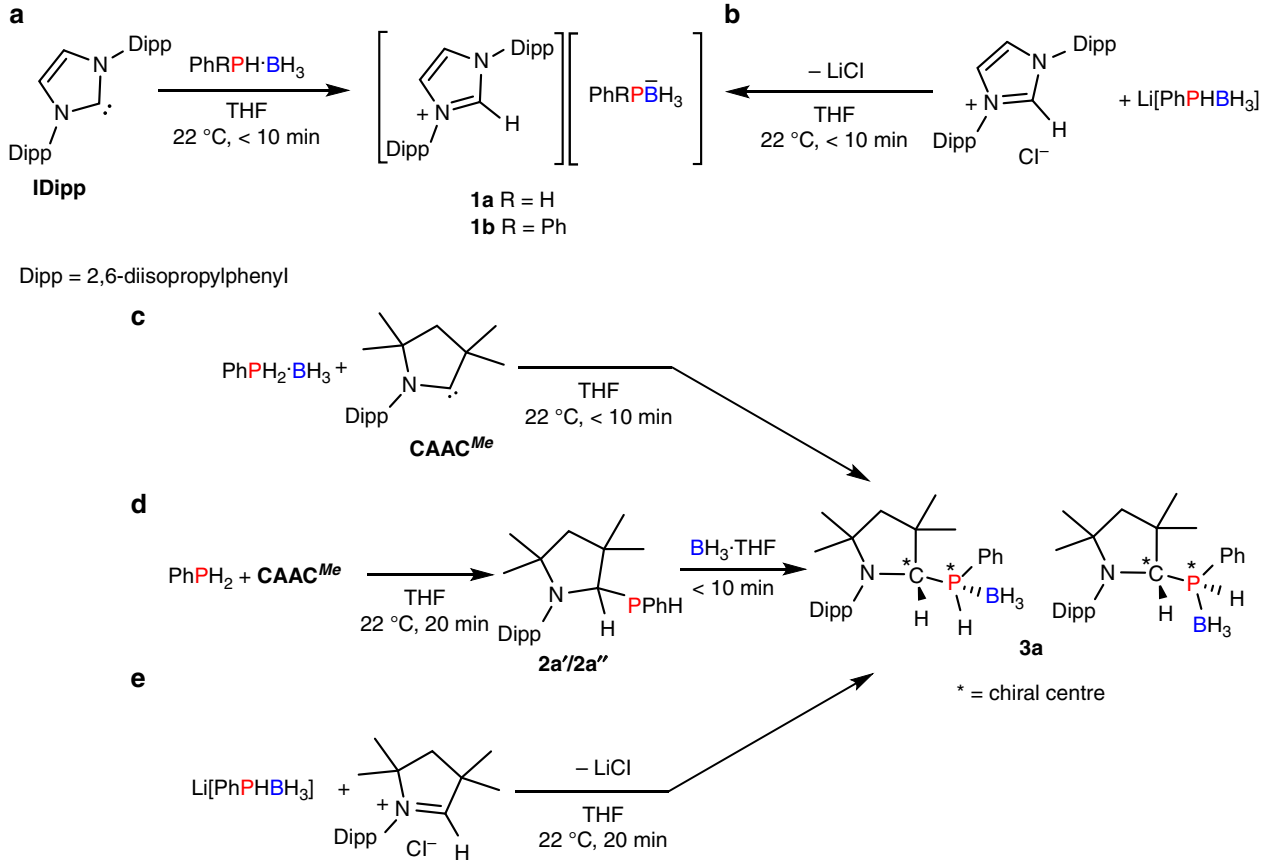

Fig. 2 Reactivity of IDipp and CAAC^{Me} with phosphine-boranes. **a** Synthesis of **1a** and **1b** by deprotonation of the phosphine-borane using IDipp; **b** synthesis of **1a** and **1b** using salt metathesis route; **c** synthesis of **3a** through oxidative addition of $PhPH_2{\cdot}BH_3$; **d** synthesis of **3a** through stepwise reaction of $PhPH_2$, then $BH_3{\cdot}THF$; and **e** synthesis of **3a** through salt metathesis route

and ^{11}B nuclear magnetic resonance (NMR) spectroscopy showed complete conversion to a new species ($\delta_P = -84.2$ppm (br), $\delta_B = -33.4$ppm (dq) in THF) (Supplementary Figs. 2 and 3). The similarity of these spectral features to those observed for $Li[PhPHBH_3]$ ($\delta_P = -93.8$ppm (d), $\delta_B = -34.6$ppm (dq) in THF)[46], an analogous compound with a different cation, is consistent with deprotonation of $PhPH_2{\cdot}BH_3$ by IDipp to yield the salt [IDippH][$PhHPBH_3$] (**1a**) (Fig. 2a). The formation of this salt was further confirmed by an independent synthesis via a metathesis reaction in THF between [IDippH]Cl and $Li[PhHPBH_3]$. This showed ^{11}B and ^{31}P NMR spectral features that matched those assigned to **1a** along with precipitation of LiCl (Fig. 2b). The ^{13}C NMR spectrum of **1a** showed no $^1J_{CP}$ couplings involving the iminium carbon atom, which, together with the downfield chemical shift in the ^1H NMR spectrum of the imidazolium proton ($\delta_H =$ 10.0ppm) (Supplementary Fig. 1), supports an ionic formulation for this species in solution. When $Ph_2PH{\cdot}BH_3$ was reacted with IDipp, the analogous salt [IDippH][Ph_2PBH_3] (**1b**) was formed (Supplementary Figs. 4–6) and subsequently characterised using X-ray crystallography (Supplementary Fig. 7 and Supplementary Table 6).

Next, we attempted the analogous reaction with a CAAC as the smaller HOMO–LUMO separation of CAACs renders them potentially better candidates for E–H bond activations. The P–H activation of $PhPH_2{\cdot}BH_3$ by one equivalent of CAAC^{Me} (Fig. 2c) occurred readily at 22 °C in THF to give **3a**, which exists as two diastereomers (**3a′** and **3a″**). The identity of **3a** was initially established based on a distinctive doublet of quartet of doublets coupling pattern observed in the ^1H NMR spectrum for the P–H protons (Supplementary Figs. 8–10). This assignment was further corroborated by an independent synthesis via a stepwise procedure involving oxidative addition of $PhPH_2$ to the carbene centre in CAAC^{Me} to yield **2a** (as a mixture of diastereomers each with indistinguishable enantiomers by NMR), followed by the addition of $BH_3{\cdot}THF$ to give **3a** (Fig. 2d). The two diastereomers of **3a** were also formed immediately upon combining $Li[PhHPBH_3]$ and [CAAC^{Me}H]Cl through elimination of LiCl (Fig. 2e). In contrast to the results obtained in the reaction of [IDippH]Cl and $Li[PhHPBH_3]$ above (Fig. 2b), the lower steric hindrance and greater π-acidity[36] of the cation [CAAC^{Me}H]$^+$ leads to the formation of a molecular species with a distinct P–C bond, rather than the corresponding iminium salt [CAAC^{Me}H][$PhHPBH_3$]. The molecular formulation of **3a** is supported by the observation of both $^1J_{CP}$ ($^1J_{CP} = 41.0$ Hz (**3a′**), $^1J_{CP} = 38.3$ Hz (**3a″**)) and $^2J_{HP}$ ($^2J_{HP} =$ 4.2 Hz (**3a′**), $^2J_{HP} = 5.8$ Hz (**3a″**)) coupling constants in the ^{13}C and ^1H NMR spectra.

Attempts to crystallographically characterise **3a** were unsuccessful as solutions in THF (0.10 M) spontaneously decomposed to a mixture of poly(phenylphosphinoborane) $[PhHPBH_2]_n$ and (CAAC^{Me})H_2 as shown by ^1H, ^{11}B and ^{31}P NMR spectroscopy. Although only sensitive to low molar mass fractions[47], electrospray ionisation-mass spectrometry (ESI-MS) confirmed the formation of $[PhHPBH_2]_n$ (up to $n = 22$) by identifying repeat units of $\Delta(m/z) = 122.05$ (molecular weight of $[PhHPBH_2] =$ 122.05 g mol^{-1}). Isolation of pure $[PhHPBH_2]_n$ was achieved through precipitation of the reaction mixture into cold (−40 °C) hexanes to remove the hydrogenated carbene, (CAAC^{Me})H_2 (Supplementary Figs. 25 and 26), which was also characterised by X-ray crystallography (Supplementary Fig. 27 and Supplementary

Table 1 Influence of temperature, solvent and concentration on the formation of poly(phenylphosphinoborane), $[PhHPBH_2]_n$, in a closed system

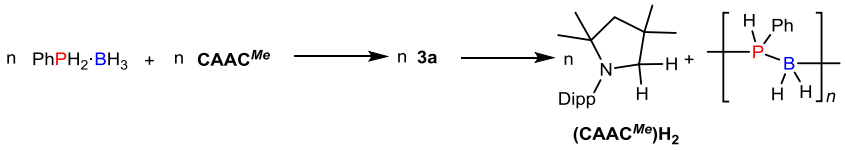

Run	Temp. (°C)	Solvent	Conc. (M)	Time (h)[a]	DP[b]	M_n (Da)[c]	PDI[c]
1	22	THF	0.50	120	205	25,000	1.55
2	60	THF	0.10	3	–[d]	–[d]	–[d]
3	60	THF	0.50	3	410	50,100	1.27
4	60	THF	1.26	3	686	83,800	1.13
5	60	Toluene	0.50	3	290	35,400	1.28
6	110	Toluene	0.50	0.5	230	28,000	1.52
7	110	None	N/A	3	302	36,800	1.39

GPC gel permeation chromatography, *THF* tetrahydrofuran, *N/A* not available, *NMR* nuclear magnetic resonance, DP degree of polymerisation, *PDI* polydispersity index
[a]Time taken for full conversion by ^{31}P NMR spectroscopy
[b]DP measured by GPC
[c]Measured using GPC analysis
[d]No high-molecular-weight material recovered after precipitation

Table 6). In the present case, the eliminated phosphinoborane monomer $[PhHPBH_2]$ polymerises, presumably due to the small size of the substituents at P and B.

The influence of temperature, solvent and concentration upon the molar mass of the poly(phenylphosphinoborane) obtained was systematically investigated with a view of optimising the polymerisation conditions (Table 1; Supplementary Table 1; and Supplementary Figs. 18–21, 23 and 24). In each case, ESI-MS and gel permeation chromatography (GPC) analyses were carried out (Supplementary Figs. 11–17, 22 and 23). ESI-MS clearly confirmed the presence of the $[PhHPBH_2]$ monomeric repeat unit in each case and allowed us to detect the presence of either BH_3 or $PPhH_2$ end groups (Supplementary Fig. 22). However, due to only the low molar mass fraction being detected by the method, it is not possible to draw links between the reaction conditions and the degree of polymerisation using these data[47]. In contrast, GPC analysis permitted optimisation of the polymerisation conditions as this technique reveals the complete molar mass distribution (Table 1 and Supplementary Table 1). Increasing the temperature (run 1 vs. 3, and 5 vs. 6) reduced the reaction time, but has no significant effect on the molar mass of the polymer obtained. Using a non-polar solvent (toluene) rather than THF (runs 3 vs. 5) also had no significant effect on the polymer molar mass. It was found that at higher concentrations (run 2 vs. 3 vs. 4), a larger quantity of polymeric relative to oligomeric material was formed (Supplementary Fig. 17). This observation is consistent with head-to-tail polymerisation of transiently generated phenylphosphinoborane, $[PhHPBH_2]$. The reaction was also attempted under solvent-free, melt conditions at 110 °C (run 7), and, although high molar mass material was formed, the molar mass was no greater than that obtained using a concentrated solution at 60 °C. Due to concerns about the homogeneity of the reaction as a result of poor mixing, subsequent studies were performed in concentrated solutions rather than in the melt phase.

Mechanistic studies. A series of experimental and density functional theory (DFT) studies have been undertaken to probe the mechanism of the dehydrogenation of $PhPH_2{\cdot}BH_3$ with $CAAC^{Me}$. Several mechanisms for the generation of monomeric $[PhHPBH_2]$ were considered and subsequently discounted, based on experimental and computational evidence (for a full discussion see 'Proposed and subsequently discounted mechanisms for phosphine-borane dehydrogenation mediated by $CAAC^{Me}$' in the Supplementary Information; Supplementary Figs. 32 and 33; and Supplementary Tables 3 and 5), before the final mechanism shown below was proposed and supported (Fig. 3). Attempts to trap the released monomer with either cyclohexene[48] or 1,3-cyclohexadiene[49] proved unsuccessful.

Kinetic studies were conducted to assess the proposed mechanisms (Supplementary Table 2 and Supplementary Fig. 28). A plot of ln[**3a**] vs. reaction time showed equivalent half-lives of 1.5 h (Supplementary Fig. 29) for several initial concentrations between 0.3 and 0.7 M at 50 °C, indicating a first-order process in **3a**. Monitoring the reaction at several temperatures between 22 and 60 °C allowed the enthalpy and entropy of activation to be calculated as 21.5 kcal mol^{-1} and −9.5 cal K^{-1} mol^{-1}, respectively, consistent with a substantial energy barrier involving a relatively ordered transition state (Supplementary Fig. 30).

DFT calculations were carried out at the PBE0/6-31 + G(d,p)/IEFPCM(THF) level of theory[50–52] with an *N*-phenyl model system for the $CAAC^{Me}$ (**B**) to further elucidate the dehydrogenation mechanism (Fig. 3). An initial deprotonation of the P–H bond of $PhPH_2{\cdot}BH_3$ (**A**) with **B** to give a $[CAAC(H)]^+$ and $[PhPH(BH_3)]^-$ ion pair ($\mathbf{C_{pair}}$) was the most favoured first reaction step with a low Gibbs free energy of activation of 4.9 kcal mol^{-1} (see 'DFT calculations' in the Supplementary Information). Subsequent nucleophilic attack at the iminium carbon of the $[CAAC(H)]^+$ cation by the phosphorus centre of the $[PhPH(BH_3)]^-$ anion leads via **TS4** to the S_P,*S* (**F**) diastereomer of the P–H activation product, or via **TS4′**, to the other R_P,*S* (**F′**) diastereomer. The calculation of the activation barrier for this step was hampered by the inherently flat progression of the potential energy hypersurface between **TS4** or **TS4′** and $\mathbf{C_{pair}}$, which suggests, in agreement with the experimentally found rapid formation of **3a**, that this step occurs with a very small activation barrier. **F** and **F′** are kinetic products of the reaction. Significantly, this step is reversible via P–C dissociation, for which a maximum activation barrier of 18.7 kcal mol^{-1} was calculated from **F** to **TS4**. This opens up a second reaction pathway from $\mathbf{C_{pair}}$ leading to $(CAAC)H_2$ (**G**) and $[PhHPBH_2]$ (**H**) via B–H hydride abstraction from the $[PhPH(BH_3)]^-$ anion by the π-acidic $(CAAC\text{-}H)^+$ cation with a low activation barrier of 5.3 kcal mol^{-1} (via **TS5**). Thus, the formation of $[PhHPBH_2]_n$ from **3a**

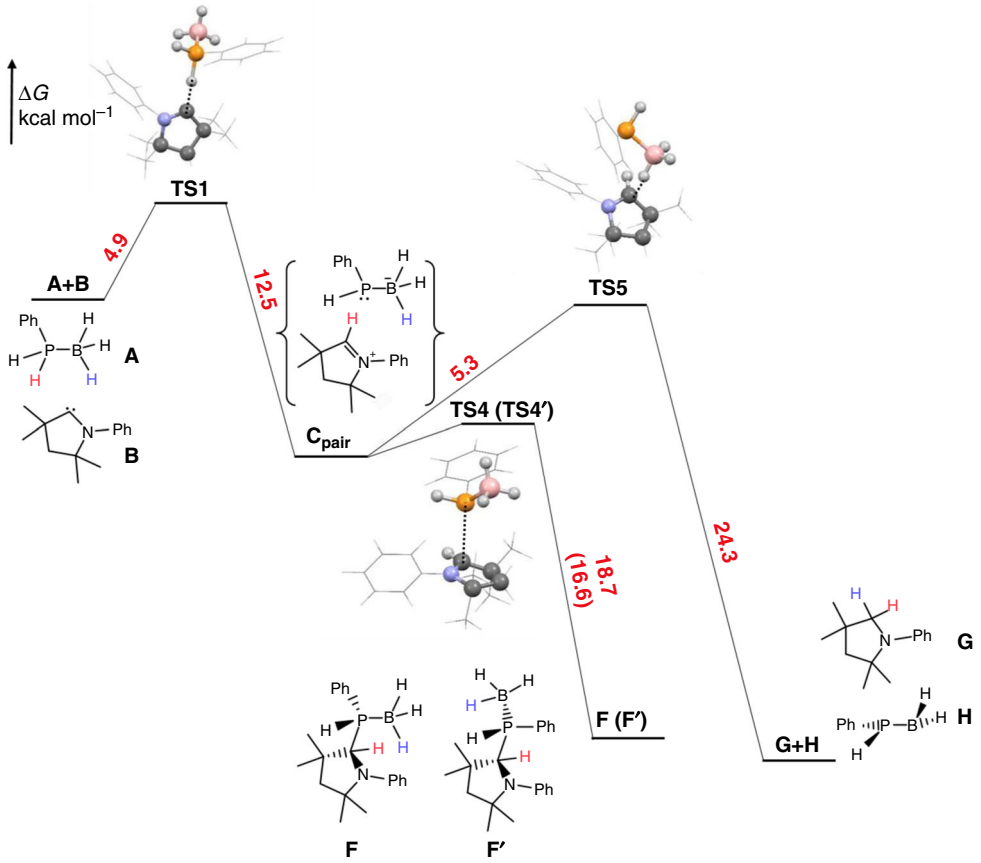

Fig. 3 DFT study. Simplified schematic reaction profile calculated for the reaction of $PhPH_2{\cdot}BH_3$ (**A**) with *N*-phenyl CAAC (**B**) at the PBE0/6-31 + G(d,p)/IEFPCM(THF) level of theory; Gibbs free energies for the second diastereomer are given in round brackets (for a comprehensive depiction of the reaction profile see Supplementary Fig. 31)

can be rationalised by the formation of transient $[CAAC(H)]^+$ and $[PhPH(BH_3)]^-$ ions via consecutive P–C bond scission and B–H hydride abstraction leading to $(CAAC^{Me})H_2$ and $[PhHPBH_2]$, the latter undergoing head-to-tail polymerisation to thermodynamically favoured $[PhHPBH_2]_n$ (Supplementary Fig. 31). For a discussion of the proposed polymerisation mechanism, see 'Supplementary discussion of the polymerisation mechanism from phosphinoborane monomers' in the Supplementary Information. The fact that the reaction between $PhPH_2{\cdot}BH_3$ and IDipp stops at the $[IDipp(H)]^+$ and $[PhPH(BH_3)]^-$ ions (Fig. 2a) can be traced back to the greater π-acidity of the $[CAAC(H)]^+$ compared to the analogous $[NHC(H)]^+$ cation, as suggested by the high exergonicity of the isodesmic reaction $[CAAC(H)]^+ + (NHC)H_2 \rightarrow [NHC(H)]^+ + (CAAC)H_2$ ($\Delta G^0 = -66.8$ kcal mol^{-1}; *N*-phenyl model systems) (Supplementary Table 4).

According to the calculations, the dissociation of the P–H activation products **F** or **F′** via the transition states **TS4** or **TS4′** requires the highest activation energy in the overall mechanism, which is in agreement with the first-order rate law found for **3a** by the kinetic measurements. In addition, the calculated enthalpy of activation for this step ($\Delta H^0 = 20.2$ (**TS4**), 19.2 (**TS4′**) kcal mol^{-1}) is in good agreement with the substantial experimentally derived enthalpy of activation for the overall reaction ($\Delta H^0 = 21.5$ kcal mol^{-1}). The higher Gibbs free energy of activation required for the dissociation of the S_P,*S* diastereomer **F** ($\Delta G^0 = 18.7$ kcal mol^{-1}) compared to the R_P,*S* diastereomer **F′** ($\Delta G^0 = 16.6$ kcal mol^{-1}) accounts for the experimentally observed faster conversion of one diastereomer during the reaction. Moreover, the observed enhanced reaction rates in THF (see Supplementary Table 2) can be rationalised by the better stabilisation of the $[CAAC(H)]^+$ and $[PhPH(BH_3)]^-$ ions in THF than in toluene, which is further corroborated by the calculations (Supplementary Fig. 31).

Substrate scope. Given the success with $PhPH_2{\cdot}BH_3$, the scope of the $CAAC^{Me}$-mediated dehydropolymerisation was extended with the aim of targeting hitherto inaccessible high molar mass P-disubstituted polyphosphinoboranes. $CAAC^{Me}(H)Ph_2PBH_3$ (**3b**) was synthesised from $Ph_2PH{\cdot}BH_3$ and $CAAC^{Me}$ in THF (Fig. 4a and Supplementary Figs. 34 and 35). Formation of **3b** was also detected immediately upon combining $Li[Ph_2PBH_3]$ and $[CAAC^{Me}H]Cl$, and also through the stepwise addition of Ph_2PH followed by $BH_3{\cdot}THF$ to a solution of $CAAC^{Me}$.

Heating a concentrated solution of **3b** (2.5 M, 60 °C, 1 h, THF or toluene) effected complete conversion to $(CAAC^{Me})H_2$, the linear dimer $Ph_2PHBH_2PPh_2BH_3$, cyclic oligomers $[Ph_2PBH_2]_x$ ($x = 3, 4$), and the polymer $[Ph_2PBH_2]_n$ as observed by ^1H and ^{31}P NMR (Fig. 4a and Supplementary Fig. 40a)[53]. Removal of $(CAAC^{Me})H_2$ and cyclic oligomers was achieved by precipitation into hexanes, but attempts to separate $Ph_2PHBH_2PPh_2BH_3$ and $[Ph_2PBH_2]_n$ proved unsuccessful (for details see 'Dehydropolymerisation of $Ph_2PH{\cdot}BH_3$' in the Supplementary Information). ESI-MS analysis of the product after precipitation nevertheless confirmed the presence of the repeat unit $\Delta(m/z) = 198.08$ (molecular weight of $[Ph_2PBH_2] = 198.08$ g mol^{-1}, maximum value of $n = 10$) (Supplementary Fig. 36). However, GPC analysis showed only a very small amount of high molar mass material. Interestingly, when toluene, rather than THF, is used as the solvent, a much smaller quantity of linear dimer is formed (Supplementary Figs. 37 and 40b). Under these conditions,

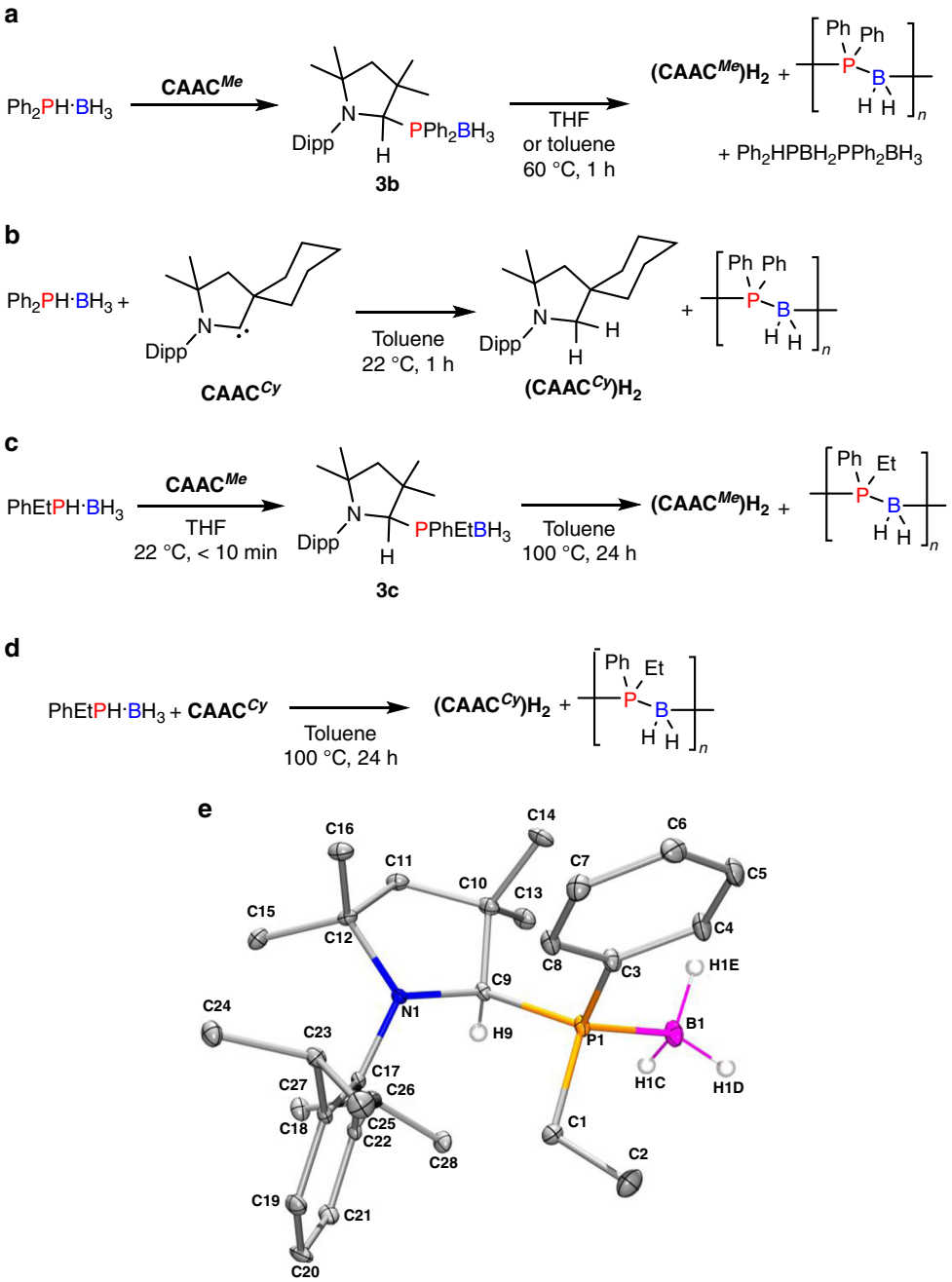

Fig. 4 Reactions of $Ph_2PH{\cdot}BH_3$ and *rac*-Ph(Et)PH·BH_3 with $CAAC^{Me}$ and $CAAC^{Cy}$. **a** $CAAC^{Me}$-mediated dehydrocoupling of $Ph_2PH{\cdot}BH_3$; **b** $CAAC^{Cy}$-mediated dehydrocoupling of $Ph_2PH{\cdot}BH_3$; **c** $CAAC^{Me}$-mediated dehydrocoupling of *rac*-Ph(Et)PH·BH_3; **d** $CAAC^{Cy}$-mediated dehydrocoupling of *rac*-Ph(Et)PH·BH_3; and **e** thermal ellipsoid plot of **3c**. H atoms other than those bound to C9 and B1 have been omitted for clarity. Ellipsoids are shown at the 30% probability level

GPC analysis on the precipitated material showed a majority of low molar mass material (M_n = ca. 1,300; polydispersity index (PDI) = 1.31) and a small amount (ca. 10%) of high molar mass material (M_n = 54,300; PDI = 1.12) (Supplementary Fig. 38).

With the aim of increasing the yield and amount of high molar mass material, we investigated the use of the more reactive $CAAC^{Cy}$, exemplified by its ability to activate dihydrogen under mild conditions[37]. The initially formed P–H activation compound is consumed within 1 h at 22 °C (Fig. 4b). However, GPC analysis again showed only a small amount (ca. 12%) of high molar mass material (M_n = 59,600; PDI = 1.08) with the majority being low molar mass material (M_n = ca. 1100; PDI = 1.28) (Supplementary Figs. 39, 40c and 41–45).

In an attempt to further extend the scope of the dehydropolymerisation to other P-disubstituted phosphine-boranes the reactivity of *rac*-Ph(Et)PH·BH_3 with $CAAC^{Me}$ and $CAAC^{Cy}$ was investigated. $CAAC^{Me}$(H)PhEtPBH_3 (**3c**) was formed through direct reaction of $CAAC^{Me}$ with *rac*-PhEtPH·BH_3 (Supplementary Figs. 46–50). Unlike with the mono- and diphenyl derivatives, **3c** is stable at 22 °C, which allowed the structure to be confirmed by X-ray diffraction (Fig. 4e and Supplementary Table 6). Upon heating isolated **3c** to 100 °C, the targeted dehydropolymerisation occurred to give $[PhEtPBH_2]_n$ and $(CAAC^{Me})H_2$ (Fig. 4c and Supplementary Fig. 51). Pure $[PhEtPBH_2]_n$ was obtained in 23% yield as a fine white powder following precipitation. ESI-MS analysis of the precipitated

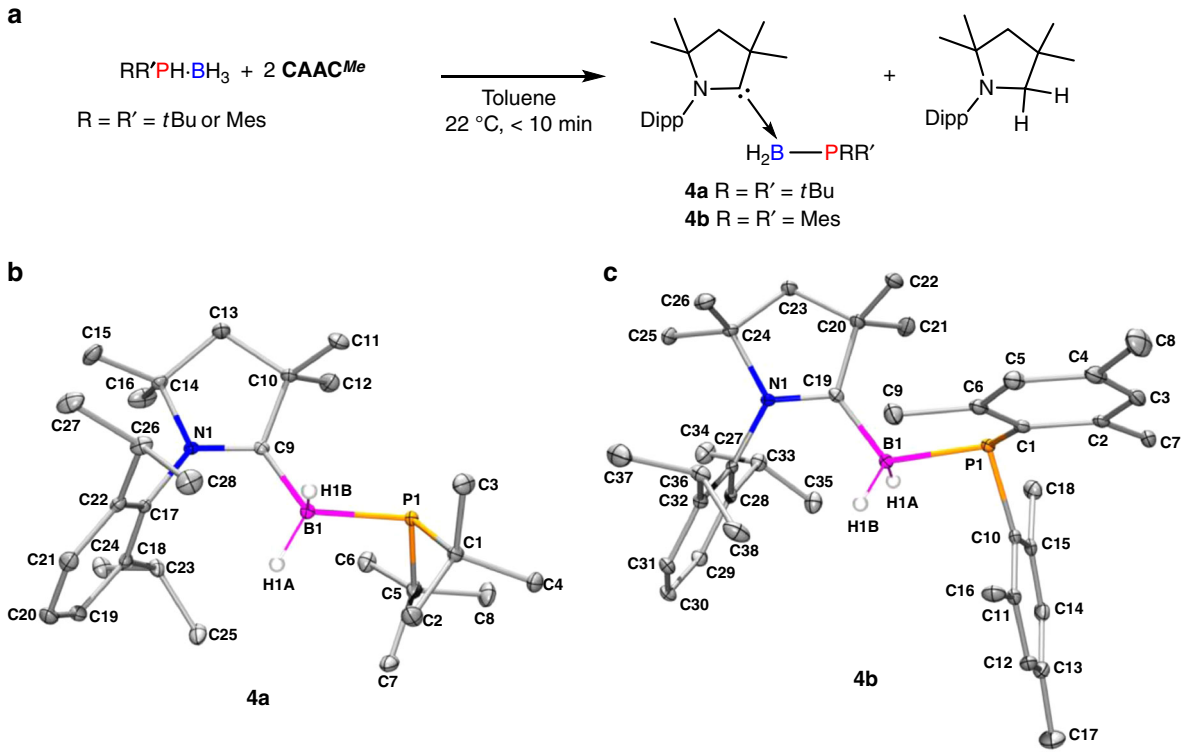

Fig. 5 Synthesis and structure of cyclic (alkyl)(amino)carbene-phosphinoborane adducts **4a** and **4b**. **a** Synthesis of **4a** and **4b**; **b** thermal ellipsoid plot of **4a**; and **c** thermal ellipsoid plot of **4b**. For both **4a** and **4b** ellipsoids are shown at the 30% probability level, and H atoms other than those at the B1 centre have been omitted for clarity

sample confirmed the presence of the repeat unit of $[PhEtPBH_2]_n$ ($\Delta(m/z) = 150.08$, molar mass of $[PhEtPBH_2] = 150.08$ g mol^{-1}) and $n = 33$ (Supplementary Fig. 52); however, there was no convincing high molar mass material observed using GPC. In the analogous reaction using CAAC^{Cy}, the yield was also low (19%); however, a GPC peak corresponding to high molar mass material ($M_n = 62{,}600$, PDI = 1.19, n = ca. 400) was observed (Supplementary Figs. 53–58). Again this was only a small amount (ca. 18 %) compared to the low molar mass fraction (M_n = ca. 1900; PDI = 1.47, n = ca. 13). Upon closer analysis of the ESI-MS spectra for each synthesis of $[Ph_2PBH_2]_n$ and $[PhEtBH_2]_n$, the end group of the major distribution was detected as being either CAAC^{Me} or CAAC^{Cy} (Supplementary Figs. 36, 37, 44, 52 and 56). These results suggest that trace amounts of CAACs may react with the polymer chain at some point during the polymerisation (for further discussion see 'Supplementary discussion of the polymerisation mechanism from phosphinoborane monomers' in the Supplementary Information).

When the reactivity of CAAC^{Me} with bulkier P-disubstituted phosphine-borane substrates (R = R′ = *t*Bu or R = R′ = Mes) was explored, an enlightening divergence in reactivity was noted. For full conversion of these substrates, two equivalents of CAAC^{Me} are required. In situ ^{1}H NMR reveals that an equimolar mixture of (CAAC^{Me})H_2 and the new species **4a**/**4b** are formed (Fig. 5a and Supplementary Figs. 59–68).

The structures of **4a** and **4b** were confirmed by X-ray crystallography revealing that in both compounds the CAAC^{Me} C-donor was bound to the boron of the phosphinoborane moiety (Fig. 5b, c and Supplementary Table 7). Interestingly, species **4a** and **4b** are analogous to the previously mentioned NHC–phosphinoborane adducts that have been recently reported[45].

The reactivity with the bulky, P-disubstituted phosphine-boranes contrasts with that observed with $PhPH_2{\cdot}BH_3$, $Ph_2PH{\cdot}BH_3$ and $PhEtPH{\cdot}BH_3$ as an initial P–H oxidative-addition product analogous to compounds **3a–c** is not observed. The monomeric phosphinoborane generated upon dehydrogenation does not undergo head-to-tail polymerisation, instead it is trapped by a second equivalent of carbene. The absence of an observable P–H activation compound can be explained by the greater steric bulk around the phosphorus centre. The trapping, however, provides further evidence for the release of monomeric phosphinoboranes in the proposed polymerisation mechanism. It is noteworthy that when $Ph_2PH{\cdot}BH_3$ is reacted with two equivalents of CAAC^{Me} clean conversion to the species analogous to **4a** and **4b** is not observed; however, peaks for the short-chain oligomers CAAC$(BH_2PPh_2)_x$ (x = 1–4) have been identified using ESI-MS (Supplementary Fig. 69).

Discussion

In summary, we have shown that cyclic alkyl(amino)carbenes can be used as stoichiometric reagents to effect P–H/B–H dehydrogenative coupling of primary and secondary phosphine-boranes. These results illustrate the complementarity between organic and transition metal ambiphiles in the context of the main-group redox transformations, and hint at a potentially broad utility for CAACs in accessing new inorganic polymers and materials. The carbene centre in CAAC^{Me} inserts into the P–H bond of phosphine-boranes, RR′PH·BH_3 (R = Ph; R′ = H, Ph, or Et), to give derivatives of CAAC^{Me}(H)PRR′BH_3 (**3a–c**) which undergo thermolysis to give the hydrogenated carbene (CAAC^{Me})H_2 and polymers $[RR'PBH_2]_n$. Most remarkable is that in the case of $Ph_2PH{\cdot}BH_3$ with CAAC^{Cy} the dehydropolymerisation proceeds within 1 h at 22 °C. In contrast, with respect to the reactivity of sterically encumbered P-disubstituted phosphine-boranes (R = R′ = *t*Bu or Mes) with CAAC^{Me}, it is noteworthy that polymers are not generated post H_2 transfer. Instead, the transient phosphinoboranes were trapped by a second equivalent of carbene to yield

CAAC^{Me}–phosphinoborane adducts, **4a** and **4b**. The novel dehydropolymerisation using CAACs has been used to prepare samples of P-disubstituted polyphosphinoboranes, $[Ph_2PBH_2]_n$ and $[PhEtPBH_2]_n$, which cannot be accessed via previous transition metal-catalysed or stoichiometric routes, and contain high molar mass fractions. The development of catalytic rather than stoichiometric reactions involving main-group species is a rapidly developing field[54,55]. The reactions of phosphine-boranes with species that undergo E–H bond activation, for example, stannylenes[56] and frustrated Lewis pairs that reversibly bind H_2[57,58], are under current investigation. Future studies will target the generation of a well-defined propagating site, which should allow access to predominantly linear polymers, molar mass control and potentially block copolymers. A more atom-economic catalytic synthesis would also allow a more facile scale-up and thereby the properties of the new materials to be investigated in detail.

Methods

Detailed procedure for polymerisation of $PhPH_2{\cdot}BH_3$ using CAAC^{Me} (run 4). $PhPH_2{\cdot}BH_3$ (156 mg, 1.26 mmol) and CAAC^{Me} (360 mg, 1.26 mmol) were dissolved in THF (1 mL) in a J. Young Schlenk tube, sealed and the reaction mixture was stirred at 60 °C for 3 h. The reaction mixture was added dropwise into 20 mL of rapidly stirred cold hexanes at −40 °C, yielding a precipitate, and the supernatant was decanted. The precipitation was repeated twice more prior to drying in vacuo to leave a white powder of the $[PhHPBH_2]_n$ polymer product. Yield (precipitated material) = 42 mg (27%). GPC (2 mg mL^{-1}): M_n = 83,800 Da; PDI = 1.17. Full experimental details for all polymerisations can be found in the Supplementary Methods.

Data availability

Crystallographic data for the structures reported in this article have been deposited at the Cambridge Crystallographic Data Centre, under deposition nos. CCDC 1867656–1867660.

Received: 2 October 2018 Accepted: 5 February 2019
Published online: 26 March 2019

References

1. Jäkle, F. Advances in the synthesis of organoborane polymers for optical, electronic, and sensory applications. *Chem. Rev.* **110**, 3985–4022 (2010).
2. Priegert, A. M., Rawe, B. W., Serin, S. C. & Gates, D. P. Polymers and the *p*-block elements. *Chem. Soc. Rev.* **45**, 922–953 (2016).
3. He, X. & Baumgartner, T. Conjugated main-group polymers for optoelectronics. *RSC Adv.* **3**, 11334–11350 (2013).
4. Jäkle, F. & Vidal, F. Functional polymeric materials based on main group elements. *Angew. Chem. Int. Ed.* https://doi.org/10.1002/anie.201810611 (2018).
5. Fazen, P. J. et al. Synthesis, properties, and ceramic conversion reactions of polyborazylene. A high-yield polymeric precursor to boron nitride. *Chem. Mater.* **7**, 1942–1956 (1995).
6. Chivers, T. & Manners, M. *Inorganic Rings and Polymers of the p-Block Elements* (Royal Society of Chemistry, London, 2009).
7. Tsang, C.-W., Yam, M. & Gates, D. P. The addition polymerization of a P=C bond: a route to new phosphine polymers. *J. Am. Chem. Soc.* **125**, 1480–1481 (2003).
8. Pavelka, L. C., Holder, S. J. & Baines, K. M. Addition polymerization of 1,1-dimesitylneopentylgermene: synthesis of a polygermene. *Chem. Commun.* 2346–2348 (2008).
9. He, G. et al. The marriage of metallacycle transfer chemistry with Suzuki−Miyaura cross-coupling to give main group element-containing conjugated polymers. *J. Am. Chem. Soc.* **135**, 5360–5363 (2013).
10. Leitao, E. M., Jurca, T. & Manners, I. Catalysis in service of main group chemistry offers a versatile approach to *p*-block molecules and materials. *Nat. Chem.* **5**, 817–829 (2013).
11. Linshoeft, J. et al. Highly tin-selective Stille coupling: synthesis of a polymer containing a stannole in the main chain. *Angew. Chem. Int. Ed.* **53**, 12916–12920 (2014).
12. McKeown, G. R. et al. Synthesis of macrocyclic poly(3-hexylthiophene) and poly(3-heptylselenophene) by alkyne homocoupling. *ACS Macro Lett.* **5**, 1075–1079 (2016).
13. Matsumura, Y. et al. Arsole-containing π-conjugated polymer by the post-element-transformation technique. *Angew. Chem. Int. Ed.* **55**, 15040–15043 (2016).
14. Adams, G. M. et al. Dehydropolymerization of $H_3B{\cdot}NMeH_2$ to form polyaminoboranes using [Rh(Xantphos-alkyl)] catalysts. *J. Am. Chem. Soc.* **140**, 1481–1495 (2018).
15. Melen, R. L. Dehydrocoupling routes to element-element bonds catalysed by main group compounds. *Chem. Soc. Rev.* **45**, 775–788 (2016).
16. Johnson, H. C., Hooper, T. N. & Weller, A. S. In *Synthesis and Application of Organoboron Compounds*, Vol. 49 (eds Fernandez, E. & Whiting, A.) 153–220 (Springer, Springer International Publishing, New York, 2015).
17. Colebatch, A. L. & Weller, A. S. Amine-borane dehydropolymerization: challenges and opportunities. *Chem. Eur. J.* **25**, 1379–1390 (2019).
18. Tilley, D. T. The coordination polymerization of silanes to polysilanes by a 'σ-bond metathesis' mechanism. Implications for linear chain growth. *Acc. Chem. Res.* **26**, 22–29 (1993).
19. Imori, T., Lu, V., Cai, H. & Tilley, T. D. Metal-catalyzed dehydropolymerization of secondary stannanes to high molecular weight polystannanes. *J. Am. Chem. Soc.* **117**, 9931–9940 (1995).
20. Choffat, F. et al. Synthesis and characterization of linear poly(dialkylstannane)s. *Macromolecules* **40**, 7878–7889 (2007).
21. Parshall, G. W. *The Chemistry of Boron and Its Compounds* (Wiley, New York, 1967).
22. Mayer-Gall, T., Knittel, D., Gutmann, J. S. & Opwis, K. Permanent flame retardant finishing of textiles by allyl-functionalized polyphosphazenes. *ACS Appl. Mater. Interfaces* **7**, 9349–9363 (2015).
23. Priegert, A. M., Siu, P. W., Hu, T. Q. & Gates, D. P. Flammability properties of paper coated with poly (methylenephosphine), an organophosphorus polymer. *Fire Mater.* **39**, 647–657 (2015).
24. Burg, A. B. Phosphinoborine polymer rings and chains from tetramethylbiphosphine. *J. Inorg. Nucl. Chem.* **11**, 258 (1959).
25. Wagner, R. I. & Caserio, F. F. Linear phosphinoborane polymers. *J. Inorg. Nucl. Chem.* **11**, 259 (1959).
26. Dorn, H., Singh, R. A., Massey, J. A., Lough, A. J. & Manners, I. Rhodium-catalyzed formation of phosphorus-boron bonds: synthesis of the first high molecular weight poly(phosphinoborane). *Angew. Chem. Int. Ed.* **38**, 3321–3323 (1999).
27. Pandey, S., Lönnecke, P. & Hey-Hawkins, E. Phosphorus-boron-based polymers obtained by dehydrocoupling of ferrocenylphosphine–borane adducts. *Eur. J. Inorg. Chem.* **2014**, 2456–2465 (2014).
28. Cavaye, H. et al. Primary alkylphosphine-borane polymers: synthesis, low glass transition temperature, and a predictive capability thereof. *Macromolecules* **50**, 9239–9248 (2017).
29. Paul, U. S. D., Braunschweig, H. & Radius, U. Iridium-catalysed dehydrocoupling of aryl phosphine–borane adducts: synthesis and characterisation of high molecular weight poly(phosphinoboranes). *Chem. Commun.* **52**, 8573–8576 (2016).
30. Schäfer, A. et al. Iron-catalyzed dehydropolymerization: a convenient route to poly(phosphinoboranes) with molecular-weight control. *Angew. Chem. Int. Ed.* **54**, 4836–4841 (2015).
31. Marquardt, C. et al. Metal-free addition/head-to-tail polymerization of transient phosphinoboranes, $RPH{-}BH_2$: a route to poly (alkylphosphinoboranes). *Angew. Chem. Int. Ed.* **54**, 13782–13786 (2015).
32. Stauber, A. et al. A convenient route to monoalkyl-substituted phosphanylboranes ($HRP{-}BH_2{-}NMe_3$): prospective precursors to poly [(alkylphosphino)boranes]. *Eur. J. Inorg. Chem.* **2016**, 2684–2687 (2016).
33. Lavallo, V., Canac, Y., Präsang, C., Donnadieu, B. & Bertrand, G. Stable cyclic (alkyl)(amino)carbenes as rigid or flexible, bulky, electron-rich ligands for transition-metal catalysts: a quaternary carbon atom makes the difference. *Angew. Chem. Int. Ed.* **44**, 5705–5709 (2005).
34. Jazzar, R. et al. Intramolecular 'hydroiminiumation' of alkenes: application to the synthesis of conjugate acids of cyclic alkyl amino carbenes (CAACs). *Angew. Chem. Int. Ed.* **46**, 2899–2902 (2007).
35. Bertrand, G. & Soleilhavoup, M. Cyclic (alkyl)(amino) carbenes (CAACs): stable carbenes on the rise. *Acc. Chem. Res.* **48**, 256–266 (2015).
36. Melaimi, M., Jazzar, R., Soleilhavoup, M. & Bertrand, G. Cyclic (alkyl)(amino) carbenes (CAACs): recent developments. *Angew. Chem. Int. Ed.* **56**, 10046–10068 (2017).
37. Frey, G. D., Lavallo, V., Donnadieu, B., Schoeller, W. W. & Bertrand, G. Facile splitting of hydrogen and ammonia by nucleophilic activation at a single carbon center. *Science* **316**, 439–441 (2007).
38. Frey, G. D., Masuda, J. D., Donnadieu, B. & Bertrand, G. Activation of Si-H, B-H, and P-H bonds at a single nonmetal center. *Angew. Chem. Int. Ed.* **49**, 9444–9447 (2010).
39. Mohapatra, C. et al. Insertion of cyclic alkyl(amino) carbene into the Si−H bonds of hydrochlorosilanes. *Inorg. Chem.* **55**, 1953–1955 (2016).

40. Turner, Z. R. Chemically non-innocent cyclic (alkyl)(amino) carbenes: ligand rearrangement, C-H and C-F bond activation. *Chem. Eur. J.* **22**, 11461–11468 (2016).
41. Jin, L. et al. Isolation of cationic and neutral (allenylidene)(carbene) and bis (allenylidene)gold complexes. *Chem. Sci.* **7**, 150–154 (2016).
42. Li, Y. et al. Acyclic germylones: congeners of allenes with a central germanium atom. *J. Am. Chem. Soc.* **135**, 12422–12428 (2013).
43. Sabourin, K. J., Malcolm, A. C., McDonald, R., Ferguson, M. J. & Rivard, E. Metal-free dehydrogenation of amine–boranes by an *N*-heterocyclic carbene. *Dalt. Trans.* **42**, 4625–4632 (2013).
44. Stubbs, N. E., Jurca, T., Leitao, E. M., Woodall, C. H. & Manners, I. Polyaminoborane main chain scission using *N*-heterocyclic carbenes; formation of donor-stabilised monomeric aminoboranes. *Chem. Commun.* **49**, 9098–9100 (2013).
45. Marquardt, C. et al. Depolymerization of poly(phosphinoboranes): from polymers to Lewis base stabilized monomers. *Chem. Eur. J.* **24**, 360–363 (2018).
46. Jaska, C. A., Lough, A. J. & Manners, I. Linear hybrid aminoborane/phosphinoborane chains: synthesis, proton-hydride interactions, and thermolysis behavior. *Inorg. Chem.* **43**, 1090–1099 (2004).
47. Staubitz, A. et al. Catalytic dehydrocoupling/dehydrogenation of *N*-methylamine-borane and ammonia-borane: synthesis and characterization of high molecular weight polyaminoboranes. *J. Am. Chem. Soc.* **132**, 13332–13345 (2010).
48. Metters, O. J. et al. Generation of aminoborane monomers $RR'N{=}BH_2$ from amine-boronium cations $[RR'NH\text{-}BH_2L]^+$: metal catalyst-free formation of polyaminoboranes at ambient temperature. *Chem. Commun.* **50**, 12146–12149 (2014).
49. Breunig, J. M., Hübner, A., Bolte, M., Wagner, M. & Lerner, H.-W. Reactivity of phosphaboradibenzofulvene toward hydrogen, acetonitrile, benzophenone, and 2,3-dimethylbutadiene. *Organometallics* **32**, 6792–6799 (2013).
50. Frisch, M. J. et al. *Gaussian 09, Revision D.01*. (Gaussian, Wallingford, 2009).
51. Adamo, C. & Barone, B. Toward reliable density functional methods without adjustable parameters: the PBE0 model. *J. Chem. Phys.* **110**, 6158–6170 (1999).
52. Hehre, W. J., Ditchfield, R. & Pople, J. A. Self-consistent molecular orbital methods. XII. Further extensions of gaussian-type basis sets for use in molecular orbital studies of organic molecules. *J. Chem. Phys.* **56**, 2257–2261 (1972).
53. Dorn, H. et al. Transition metal-catalyzed formation of phosphorus-boron bonds: a new route to phosphinoborane rings, chains, and macromolecules. *J. Am. Chem. Soc.* **122**, 6669–6678 (2000).
54. Weetman, C. & Inoue, S. The road travelled: after main-group elements as transition metals. *ChemCatChem* **10**, 4213–4228 (2018).
55. Hong, M., Chen, J. & Chen, E. Y.-X. Polymerization of polar monomers mediated by main-group Lewis acid−base pairs. *Chem. Rev.* **118**, 10551–10616 (2018).
56. Protchenko, A. V. et al. Enabling and probing oxidative addition and reductive elimination at a group 14 metal center: cleavage and functionalization of E-H bonds by a bis(boryl)stannylene. *J. Am. Chem. Soc.* **138**, 4555–4564 (2016).
57. Mo, Z., Rit, A., Campos, J., Kolychev, E. L. & Aldridge, S. Catalytic B-N dehydrogenation using frustrated Lewis pairs: evidence for a chain-growth coupling mechanism. *J. Am. Chem. Soc.* **138**, 3306–3309 (2016).
58. Boudjelel, M. et al. Catalytic dehydrogenation of (di)amine-boranes with a geometrically constrained phosphine-borane Lewis pair. *ACS Catal.* **8**, 4459–4464 (2018).

Acknowledgements

N.L.O. acknowledges the EPSRC for funding. S.S.C. and V.T.A. acknowledge the Government of Canada for Banting and NSERC postdoctoral fellowships, respectively. V.T.A. is grateful to the European Union for a Marie Curie Fellowship (H2020-MSCA-IF-2016_748371). M.I.A. thanks the Alexander von Humboldt foundation for a Feodor Lynen research fellowship. I.M. thanks the Government of Canada for a Canada 150 Research Chair.

Author contributions

N.L.O., S.S.C. and I.M. devised the project. N.L.O. and V.T.A. performed the synthetic work. V.T.A. and H.A.S. performed the X-ray crystallographic studies. M.I.A. performed the computational studies. N.L.O., S.S.C., V.T.A., M.I.A. and I.M. contributed to the analysis of the results and co-wrote the paper.

Additional information

Supplementary Information accompanies this paper at https://doi.org/10.1038/s41467-019-08967-8.

Competing interests: The authors declare no competing interests.

Reprints and permission information is available online at http://npg.nature.com/reprintsandpermissions/

Journal peer review information: *Nature Communications* thanks the anonymous reviewers for their contribution to the peer review of this work.

Publisher's note: Springer Nature remains neutral with regard to jurisdictional claims in published maps and institutional affiliations.

Open Access This article is licensed under a Creative Commons Attribution 4.0 International License, which permits use, sharing, adaptation, distribution and reproduction in any medium or format, as long as you give appropriate credit to the original author(s) and the source, provide a link to the Creative Commons license, and indicate if changes were made. The images or other third party material in this article are included in the article's Creative Commons license, unless indicated otherwise in a credit line to the material. If material is not included in the article's Creative Commons license and your intended use is not permitted by statutory regulation or exceeds the permitted use, you will need to obtain permission directly from the copyright holder. To view a copy of this license, visit http://creativecommons.org/licenses/by/4.0/.

© The Author(s) 2019